EXPERIMENTAL AND NUMERICAL INVESTIGATION OF STRUCTURAL RESPONSE OF REINFORCED CONCRETE BEAMS STRENGTHENED WITH ANCHORED FRPS

by

C. Demakos[(1)], **C. Repapis**[(2)] and **D. Drivas**[(3)]

[(1)] Professor, MEng PhD,
Reinforced Concrete Lab,
Department of Civil Engineering,
Technological Education Institution of Piraeus,
250 Thivon and Petrou Ralli str.,
122 44 Aigaleo, Athens,
Greece
☺ cdem@teipir.gr
URL: http://civil.teipir.gr/

[(2)] Research Engineer, MEng PhD,
Research Fellow, Department of Civil Engineering, Technological Education Institution of Piraeus,
☺ crepapis@teipir.gr

[(3)] Research Engineer, MEng,
Research Fellow, Reinforced Concrete Lab, Department of Civil Engineering, Technological Education Institut**ion** of Piraeus**,**
☺ dimdrivas@yahoo.gr

Abstract

The response of simply supported lightly reinforced concrete (RC) beams under monotonic loading is experimentally and numerically investigated. The beams are loaded in four-point bending with two external vertical concentrated loads. They are reinforced with longitudinal and transverse reinforcement and strengthened with carbon (CFRP) or glass (GFRP) fabrics. While experimental methods of investigation are extremely useful in obtaining information about the behaviour of reinforced concrete, the use of numerical models helps in developing a good understanding of the behaviour at lower cost.

In this study ANSYS finite element program is used to numerically verify the response of the RC beams obtained experimentally. ANSYS Solid65 nonlinear concrete solid elements are used to model the concrete, while LINK180 elements are used to model longitudinal and transverse steel reinforcement and Shell43 elements for the FRPs. The material characteristics used in the nonlinear analyses are obtained experimentally. The numerical results obtained are in good agreement with the experimental. The load capacity of the beams is within 10% of the experimental values and the failure modes and crack patterns are in good agreement with the experimental.

Keywords: *Reinforced concrete, FRP, finite element model, ANSYS*

1 Introduction

The need to strengthen RC structures is encountered in cases of load increase or damage induced to the structural members by a seismic or other action and in cases of design and construction faults. Various techniques can be applied to overcome such a structural deficiency resulting to a partial repair or complete replacement of the structure damaged. The use of FRP materials for structural repairing presents several advantages such as the high strength to weight ratio of FRP, the ease of FRPs application on site due to little equipment needed and finally the improved durability and corrosion resistance in strengthened structures. Externally bonded FRP laminates and fabrics can be used to increase shear and flexural strength of reinforced beams and columns. In order to increase flexural strength of beams, a continuous sheet of FRP can be bonded at its bottom face.

The behaviour of reinforced concrete elements is observed mainly from experiments. However, experiments take considerably time, labour and great cost and consequently, the studies are limited. A large number of finite element analysis programs have been developed over the past years in order to investigate the behaviour of reinforced concrete (RC) elements. Many of the FEA packages have difficulties in modelling the nonlinear behaviour of concrete structures adequately. The applicability of the FE models of different packages has been investigated by a great number of researchers (Cotsovos *et al.*, 2009).

In this study ANSYS (2006) is chosen for the numerical evaluation of RC beams strengthened with FRP composites. The use of ANSYS for the modelling of RC beams has been reported to be satisfactory by many researchers in the past (Barbosa and Ribeiro, 1998; Kachlakev *et al.*,, 2001; Fanning, 2001; Elyasian *et al.*, 2006; Ameli *et al.*, 2007; Santhakumar *et al.*, 2007; Sandarraja and Rajamohan, 2008; Ibrahim and Mahmood, 2009; Cotsovos *et al.*, 2009; Buyukkaragoz, 2010).

The aim of the present study was the numerical evaluation and verification of structural behavior of tested reinforced concrete beams and strengthened with FRP composites. The experimental study was on the whole executed in the Laboratory of Reinforced Concrete at Piraeus TEI (Demakos, 2008). The numerical models applied in this study provide results close to the experimental results (Demakos, 2008) obtained from five simply supported beams. The load-deflection curves obtained from numerical analyses, were compared with the reported experimental load-deflection plots in order to validate the model. The crack patterns in the beams at different loadings are also plotted. After the calibration of the model, it can then be used to extend the experimental results and study the behaviour of other beams at much lower effort, cost and much quicker, without having to conduct many experimental tests.

2 Numerical modelling with ANSYS

ANSYS (version 11) (2006) finite element program was chosen for the numerical evaluation of RC beams strengthened with FRP composites. Concrete is a material

presenting nonlinear behaviour during loading and it was modelled with ANSYS to show similar behaviour.

2.1 Concrete

Solid65 element was used to model the concrete. This element is used for the 3-D modelling of solids with or without reinforcing bars (rebar). The solid is capable of cracking in tension and crushing in compression. The William and Warnke (1975) failure criterion is used for both cracking and crushing failure modes through a smeared model.

The element is defined by eight nodes and the isotropic material properties. Each node has three degrees of freedom, translations in the nodal x, y, and z directions. Up to three different rebar specifications may be defined. In our study reinforcement was modelled as another element.

Shear transfer coefficient represents conditions of the crack face. This coefficient represents a shear strength reduction factor for those subsequent loads, which induce sliding (shear) across the crack face. A value β_t for an open crack and β_c for a closed crack are given. The value of shear transfer coefficient ranges from 0.0 to 1.0. A value of 0.0 represents a smooth crack with complete loss of shear transfer, while 1.0 represents a rough crack with no loss of shear transfer. The values used in many studies varied. Santhakumar *et al.* (2007) for beams under pure bending used a value of 0.2 for open crack and 0.22 for closed crack, as proposed by *Kachlakev et al.* (2001), while for beams under combined bending and torsion used values of 0.1 and 0.12. Cotsovos *et al.* (2009) studied the effect of this parameter and concluded that adopting relatively high values, the FEA model yield realistic predictions of the response of the ductile beam investigated in their study, while adopting the same parameters to a brittle beam the FEA model overestimated the load carrying capacity and the maximum deflection. In this study a range of values for these coefficients were tested and finally an open shear transfer coefficient of 0.25 and a closed shear transfer coefficient of 0.65 were chosen. Another parameter is the tensile crack factor, which is a multiplier for amount of tensile stress relaxation, and a value of 0.6 was adopted. The crushing capability was suppressed in this study and material cracked whenever a principal stress component exceeded the tensile stress, which was taken 1.9 MPa.

2.2 Reinforcing Steel

Barbosa and Riberio (1998) modelled the same beam using Solid65 element for concrete, once adopting truss bars as discrete reinforcement connecting solid elements nodes and once composed uniquely of solid elements, some of which containing a smeared reinforcement. The results of load-deflection curves were similar. In the current study a Link180 element was used to model steel reinforcement. This 3-D spar element is a uniaxial tension-compression element with three degrees of freedom at each node, translations in the nodal x, y, and z directions. Reinforcement bars were modelled connecting the nodes of concrete solid elements. As concrete and reinforcement bars used the same nodes, a perfect bond was considered between these two materials. This assumption is made from other researchers too (Kachlakev *et al.*, 2001; Fanning, 2001; Santhakumar *et al*,. 2007).

2.3 Steel Plates

Steel plates were present at the supports and loading locations in order to avoid stress concentration problems. Steel plates were assumed to be of linear elastic material. An eight-node solid element, Solid45, was used to model the steel plates. The element is defined with eight nodes having three degrees of freedom at each node, translations in the nodal x, y, and z directions.

2.4 FRP Laminates

FRP materials consist of a large number of small, continuous, directionalized, organic (composite) fibers with advanced characteristics, embedded in a resin matrix. Depending on the type of fiber they are referred to as AFRP (aramid fiber based), CFRP (carbon fiber based) or GFRP (glass fiber based). In this study the beams were strengthened with GFRPs and CFRPs at their bottom face.

A Shell43 element was used to model the FRP composites. The element has six degrees of freedom at each node. The bond between the FRP composites and concrete was considered also to be perfect. Pham *et al*. (2006) studied the bond characteristic between CFRP and concrete. Numerical analyses without perfect bonding should be also checked in future research.

3 Numerical Analysis

Experimental results from tests made in the Laboratory (Demakos, 2008) were compared with the numerical results from ANSYS in order to validate the numerical representation of reinforced concrete beams strengthened with FRP composites.

3.1 Geometry and materials properties of beams tested

Five 1100 mm long RC beams, with an effective span of 900 mm, were designed, constructed in the Laboratory and tested under monotonic four-point bending loading (**Fig. 1)**. These beams are part of a group of specimens tested in the Laboratory (Demakos, 2008). The loading was applied stepwise through a 200 KN capacity servo-hydraulic machine in a force-controlled mode at the center of a stiffened spreader trapezoidal beam, which in turn distributed the load equally on a couple of identical bearing pads placed on the top of the beams **(Fig.2)**. The beams consist of one control beam, and four beams strengthened with glass or carbon FRP bonded fabrics at their bottom face. In two of the strengthened beams the FRP composites were anchored in their end (**Fig. 3)**.

The control beams (BV1) were designed to fail in flexure. Beams B1/GFRP and B1/CFRP were strengthened with a glass and a carbon fabric bonded at the bottom face of the beam, respectively. In beams B1/GFRP/CMAS and B1/CFRP/CMAS one U-shaped strip of the same FRP as the strengthening fabric was bonded at each end of the FRP. Through these strips, a tuft of glass fibers, the (CMAS), saturated in the epoxy resin mixture was inserted in drilled holes at every face of the beam and the (CMAS)'

protruding tips were then splayed circularly over the U-strip. Finally, the anchored U-strip was covered by a 100x100 mm patch of the same FRP. More details about the experiments and the specimens are presented by Demakos (2008).

In **Tab. 1** all beams evaluated in this study are shown. The cross section of the beams was 100 mm width and 150 mm depth, and the length of the beam tested was 1100 mm. The control beam (BV1) dimensions along with the reinforcement details are shown in **Fig. 1**. The longitudinal reinforcement was two rebars of 8 mm diameter at the bottom and two at the top of the beams. Closed stirrups of 8 mm diameter were used, spaced every 50 mm at shear spans and 150 mm at the center of the beams. Transverse reinforcement of stirrups was designed in that way to avoid brittle shear failure of beams. The position of the FRPs in the strengthened beams is shown in **Fig. 3**.

The stress-strain relation shown in **Fig. 4a** is used for concrete. Young's modulus of elasticity is taken 27.6 GPa and Poisson's ratio 0.2. Maximum stress value is assumed to be 24 MPa, near the mean value of the test results. In the ascending part of the curve, values are calculated from the formula presented by EC2. The strain corresponding to the maximum stress is assumed to be 0.002. After the peak-stress value there is a descending (strain-softening) branch until the ultimate strain of 0.0035. Beyond this value, the stress values decrease linearly until a small residual value is attained and remains constant thereafter. The maximum tensile stress of concrete is set to a value of 1.9 MPa.

The stress-strain curve for steel rebars is shown in **Fig. 4b.** and it is identical in tension and compression. Young's modulus is taken 200 GPa and Poisson's ratio 0.3. Yield stress of the rebars is 550 MPa, and ultimate stress 610 MPa, as they were obtained from the experimental results. Steel plates for supports and loading locations have a Young's modulus of 200 GPa and Poisson's ratio of 0.3.

In the present study linear elastic properties of FRP composites are assumed, as shown in **Fig. 4**. The material properties for FRP composites used in analysis of the strengthened beams are shown in **Tab. 2**. Ultimate tensile strength in primary fiber direction was taken as 550 MPa and 1100 MPa for GRFP and CFRP, respectively. Elongation at break is 2% and 1.5%, tensile modulus is 27.5 and 75 GPa for GRFP and CFRP, respectively. Laminate thickness is 1.3 mm for GFRP and 0.45 mm for CFRP. The stress-strain curves for GFRP and CFRP are shown in **Fig. 4c** and **Fig. 4d**, respectively.

The beams were analyzed using ANSYS finite element model and compared with the test results of the above specimens. In the experimental analysis (Demakos 2008) it was shown that U-strip and (CMAS) anchorage improved the load capacity and ductility of RC specimens. In the numerical analysis the U-strip was modelled for one beam but the results were similar with the beam without the (CMAS) anchorage. This was expected since perfect bonding was assumed in analyses. Hence, only beams with a FRP fabric at the bottom face were finally analyzed, and the results were compared to the experimental for beams with and without (CMAS) anchorage.

In analysis only one quarter of each beam was modelled due to transversal and longitudinal symmetry of the concrete beam and symmetry of the applied loading. With this approach the computational time and computer disk space requirements was reduced significantly. The finite element mesh and loading regions of the beams are shown in **Fig. 5**. FRP composites are modelled in the bottom face of the beam. The boundary conditions are shown in **Fig. 6**. Steel reinforcement and stirrups modelling of beams is shown in **Fig. 7**.

4 Results

4.1 Load deflection curves and failure load

The experimental and numerical load-deflection curves obtained for the beams are shown in **Fig. 8** to **Fig. 10**. In general, the load-deflection curves and the failure load from analyses are in acceptable agreement with the experimental.

The experimental and numerical load-deflection curves obtained for the, BV1, control beam are shown in **Fig. 8**. The finite element model is stiffer than the actual beam. This difference could have several explanations. The bond between steel reinforcement and concrete is assumed perfect, although in the actual beam slip of the reinforcement may occur. Microcracks are present to the concrete to some degree due to shrinkage and handling. Also, the real material properties may be slightly different during tests than the ones assumed in analyses. The failure load of the control beam is smaller than the experimental load by 6%.

In **Fig. 9** the experimental and numerical load-deflection curves for the beam strengthened with glass FRP composites are shown. Both experimental beams, with and without the U-strip are compared with the analyzed beam, which has only a FRP fabric at its bottom face, since bonding is assumed perfect in analyses. From the test results it can be seen that (CMAS) anchorage increase significantly the strength of the beam and the beam exhibit a more ductile failure mode (Demakos, 2008). The numerical results are closer to the test results of the beam with the (CMAS) anchorage. The load-deflection curve is in good agreement and the numerical failure load is larger than the experimental by 1%.

In **Fig. 10** the experimental and numerical load-deflection curves for the beam strengthened with a carbon FRP composite are shown. In this case the curve is in a good agreement and the failure load is 10% smaller than the beam with the CMAS anchorage.

In **Fig. 11** the numerical load-deflection curves obtained for the beams B1/GFRP & B1/CFRP strengthened with glass and carbon FRP are compared. The numerical curves concerning the ultimate loading are very close, unlike the experimental results. This can be explained because the FRP composites were chosen to have similar axial stiffness. The stiffness of each strengthened beam was affected by the normalized axial stiffness of FRPs, which was expressed by the product of $t_f \cdot E_f$, where t_f and E_f denotes the thickness and tensile elastic modulus of the fabric used. The stiffness of strengthened beams at their linear elastic deformation state was almost similar for both types of strengthened beams during analyses and experiments. This is theoretically verified by evaluating the axial stiffness of both fabrics used, which was found to be about the same and equal to 35 MN/m:

$$\text{Glass FRP:} \quad t_1 \cdot E_1 = 1.30 \text{ mm} \cdot 27.5 \text{ GPa} = 35.75 \text{ MN/m} \tag{1}$$

$$\text{Carbon FRP:} \quad t_2 \cdot E_2 = 0.45 \text{ mm} \cdot 75.0 \text{ GPa} = 33.75 \text{ MN/m} \tag{2}$$

4.2 Crack pattern

The crack pattern at each applied load step is monitored by ANSYS. In **Fig. 12** the crack pattern developed for the control beam BV1 at the last loading step is shown. Cracking is shown with a circle outline in the plane of the crack. Only the first crack at an intergration point is shown. In **Fig. 13** the evolution of the crack pattern developed for

the strengthened beam B1/GFRP is shown. Finally, in **Fig. 14** the crack pattern for, BV1 and B1/GFRP/CMAS. tested beams are also shown, respectively. The crack patterns of the finite element models are similar with the experimental. Flexural cracks occurred in the mid span and were followed by diagonal shear cracks near the support. The failure modes of the finite element models show good agreement with the experimental.

5 Conclusions

A numerical study was carried out for beams strengthened with FRP laminates, using finite elements adopted by ANSYS. The numerical results were in good agreement with the experimental values. The agreement between the experimental and numerical load-deflection curves as well as the failure modes and crack patterns, suggest that satisfactory prediction can be obtained with these models.

A parametric study of models with different coefficients for concrete behaviour did not increase significantly the accuracy of the results. The observed disrepancy may occur due to slight variations in the material properties taken in analysis and those attained in experiments. If more appropriate material properties are assigned in the model, the numerical study can be used to predict more precisely the behaviour of strengthened beams with FRP laminates. Bonding between rebars and concrete or FRPs and concrete may be modelled to get better results and this is part of future research of the authors.

Numerical analyses can be used to simulate the behaviour of reinforced concrete at lower cost and predict the failure process as the experimental results reveal. Nevertheless, experiments will always be necessary in obtaining information about the real behaviour of reinforced concrete and essential in order to verify the numerical models.

This study has been achieved with the financial support of the research project granted by Technological Education Institution of Piraeus. This support is gratefully acknowledged.

References

[1] Ameli M., Ronagh H.R., Dux P.F.(2007), Behavior of FRP strengthened reinforced concrete beams under torsion. *Journal of Composites for Construction,* **11(2),** 192-200.

[2] ANSYS Inc., ANSYS Release 11, User's Manual, 2006.

[3] Barbosa A.F., Ribeiro G.O.(1998), Analysis of Reinforced Concrete Structures Using Ansys Nonlinear Concrete Model, *Computational Mechanics,* Barcelona, Spain,.

[4] Büyükkaragöz A.(2010): Finite element analysis of the beam strengthened with prefabricated reinforced concrete plate. *Scientific Research and Essays*, **5 (6)**: 533-544.

[5] Cotsovos D.M. Zeris C.A. and Abbas A.A. (2009): Finite element modelling of structural concrete. *COMPDYN 2009, Proceedings of ECCOMAS Thematic Conference on Computational Methods in Structural Dynamics and Earthquake Engineering*, Rhodes, Greece.

[6] Demakos C.B. (2008): Investigating the Influence of FRP Sheet Anchorage to Structural Response of Reinforced Concrete Beams, *International Scientific Conference SynEnergy Forum,* Spetses, Greece.
[7] Elyasian I., Abdoli N., Ronagh H. (2006): Evaluation of parameters effective in FRP shear strengthening of RC beams using FE method, *Asian Journal of Civil Engineering (building and housing),* **7 (3)**, 249-257.
[8] EN 1992-1-1. Eurocode 2 (2004): *Design of concrete structures.* Part 1: General rules and rules for buildings.
[9] Fanning P. (2001): Nonlinear Models of Reinforced and Post-tensioned concrete beams, *Electronic Journal of Structural Engineering*, **2,**122-132.
[10] Ibrahim A.M., Mahmood M.Sh. (2009): Finite Element Modeling of Reinforced Concrete Beams Strengthened with FRP Laminates. *Europ. Journal. of Scientific Research,* **30 (4),** 526-541,.
[11] Kachlakev D., Miller T., Yim S., Chansawat K. and Potisuk T. (2001): Finite Element Modeling of Reinforced Concrete Structures Strengthened with FRP Laminates. *Report for Oregon Department of Transportation,* Salem.
[12] Pham H., Al-Mahaidi R., Sauma V. (2006): Modelling of CFRP concrete bond using smeared and discrete cracks, *Composite Structures,* **75,** 145-150.
[13] Santhakumar R., Dhanaraj R., Chandrasekaran E. (2007): Behaviour of retrofitted reinforced concrete beams under combined bending and torsion: A numerical study. Electronic *Journal of Structural Engineering*, **7**, 34-45.
[14] Sundarraja M.C., Rajamohan S. (2008): Flexural Strengthening Effect on RC Beams by Bonded Composite Fabrics. *Journal of Reinforced Plastics and Composites,* **27(14),** 1497-1513.
[15] Willam K. J. and Warnke E. D. (1975): Constitutive Model for the Triaxial Behavior of Concrete, *Proceedings of International Association for Bridge and Structural Engineering,* **19,** ISMES, Bergamo, Italy: 174-186.

FIGURES and TABLES

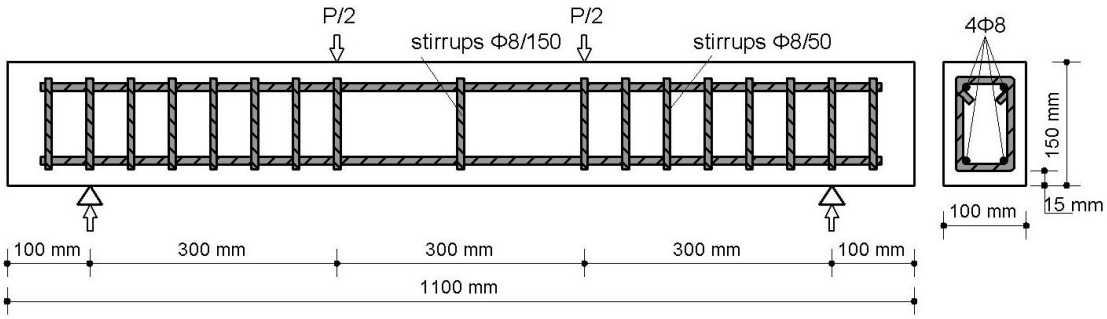

Fig. 1 Loading and geometrical properties of analysed beams (control beam BV1)

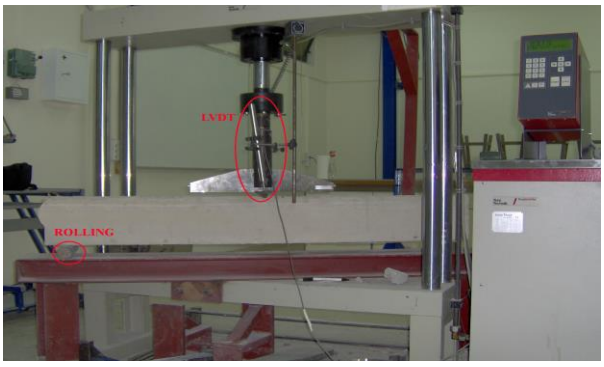

Fig. 2 Bending apparatus.

Tab. 1 Summary of tested beams evaluated in the present study

Beam	# of rebars	Stirrups (at shear spans)	External reinforcement	FRP thickness [mm]	FRP end-anchorage
BV1	4	8mm at 50mm centers	–		
B1/GFRP	4	8mm at 50mm centers	One GFRP sheet	1.30 mm	
B1/CFRP	4	8mm at 50mm centers	One CFRP sheet	0.45 mm	
B1/GFRP/CMAS	4	8mm at 50mm centers	One GFRP sheet	1.30 mm	GFRP U-strips (400mm long, extended to compression region)
B1/CFRP/CMAS	4	8mm at 50mm centers	One CFRP sheet	0.45 mm	CFRP U-strips (400mm long, extended to compression region)

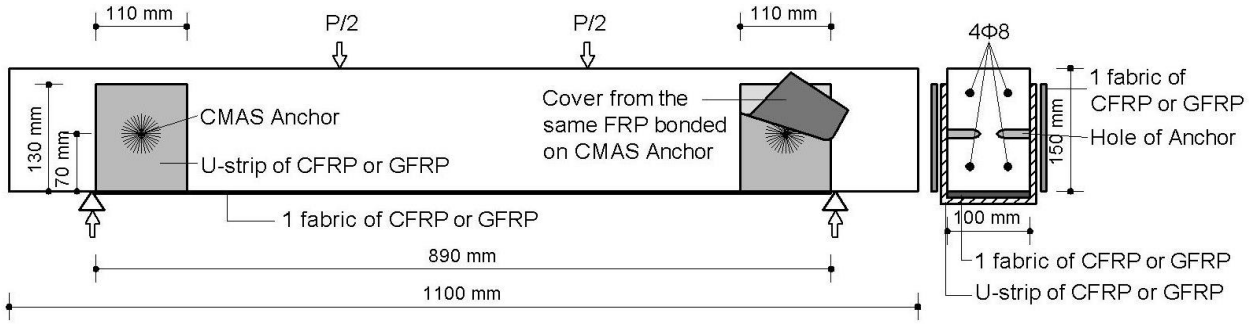

Fig. 3 Details of the composite material anchorage system (CMAS) used with FRPs in strengthened RC beam

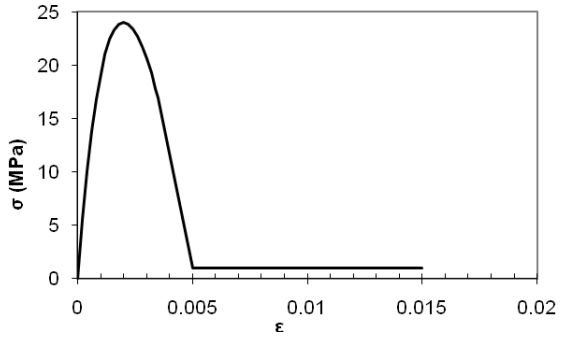

(a) Typical uniaxial compression stress-strain curve of concrete

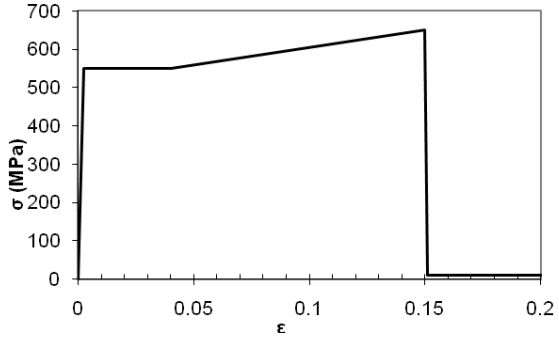

(b) Typical uniaxial stress-strain curve of steel

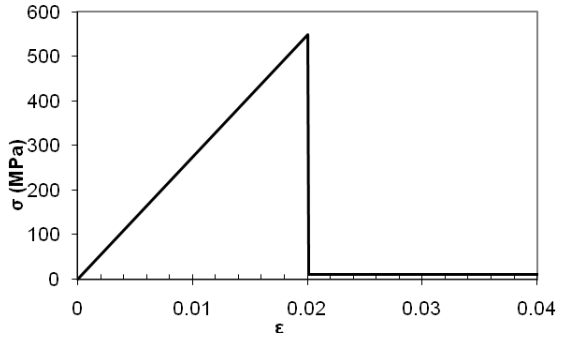

(c) Typical uniaxial tension stress-strain curve of GFRP in the direction of the fibers

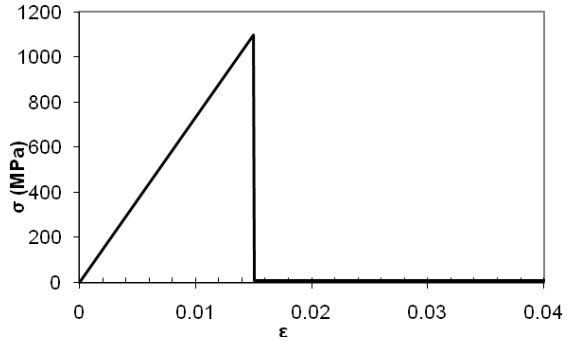

(d) Typical uniaxial tension stress-strain curve of CFRP in the direction of the fibers

Fig. 4 Material modelling behaviour with ANSYS (2006)

Tab. 2 Mechanical properties of fabrics.

Property	GFRP Composite	CFRP Composite
Ultimate tensile strength in primary fiber direction (MPa)	550	1100
Elongation at break (%)	2	1.5
Tensile modulus (GPa)	27.5	75
Laminate thickness (mm)	1.3	0.45

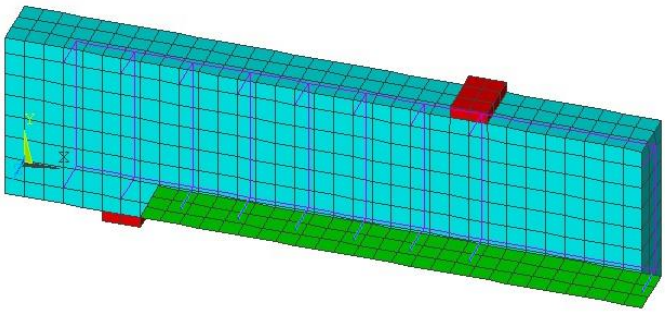

Fig. 5 Finite element mesh and loading regions for a quarter beam model

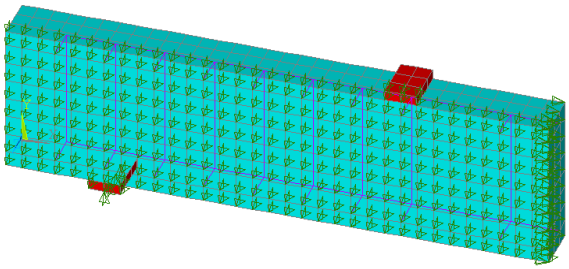

Fig. 6 Finite element mesh, boundary condition and loading regions for a quarter beam model

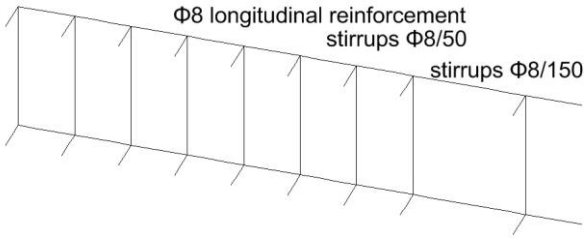

Fig. 7 Steel reinforcement and stirrups modelling of beams

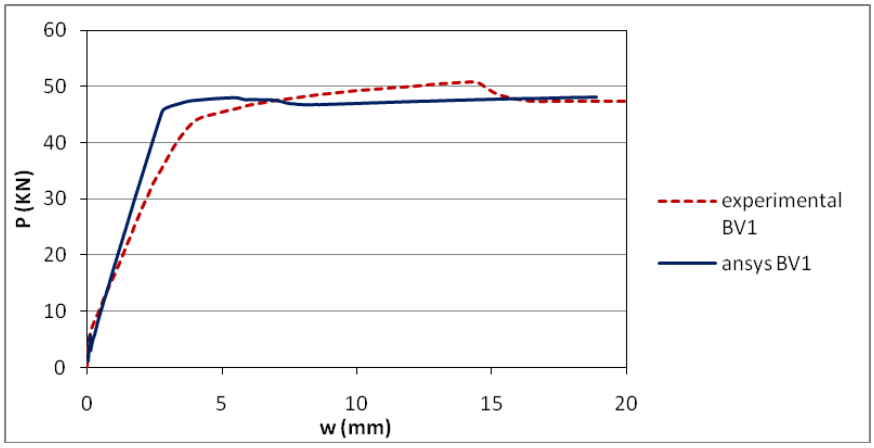

Fig. 8 Load - deflection curve for, BV1, control beam

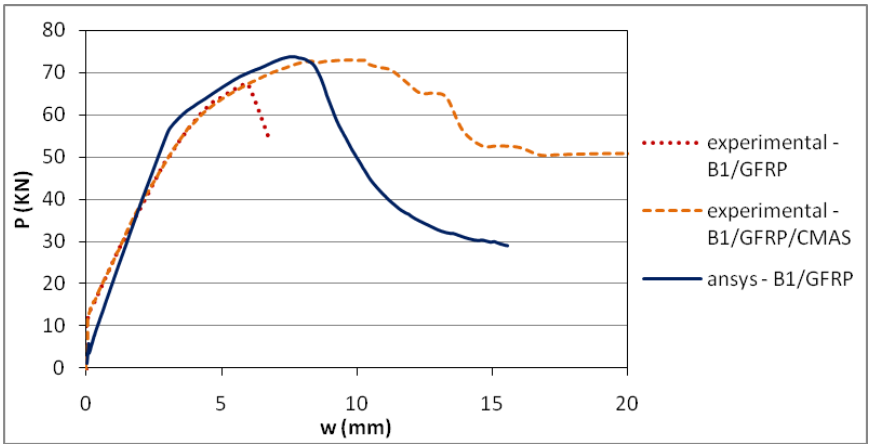

Fig. 9 Load - deflection curve for, B1/GFRP/CMAS, strengthened beam

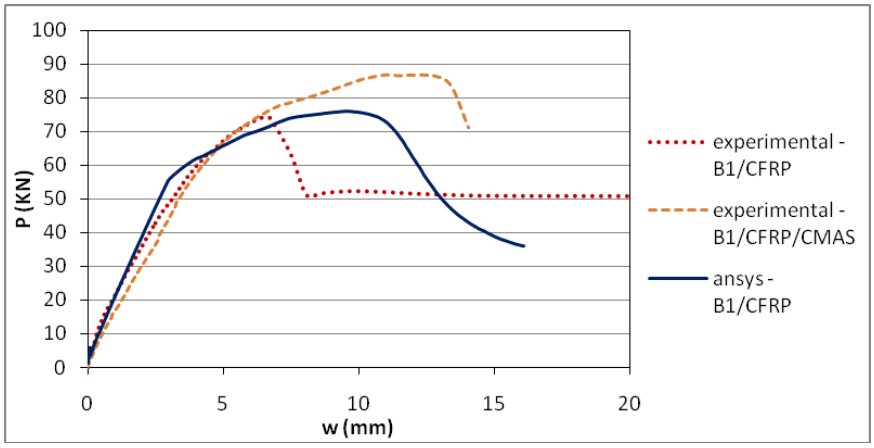

Fig. 10 Load - deflection curve for, B1/CFRP/CMAS, strengthened beam

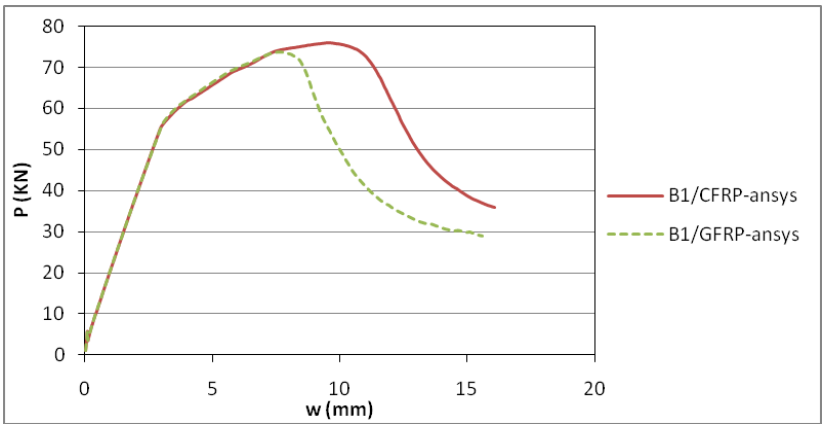

Fig. 11 Load - deflection curve for beams B1/GFRP & B1/CFRP

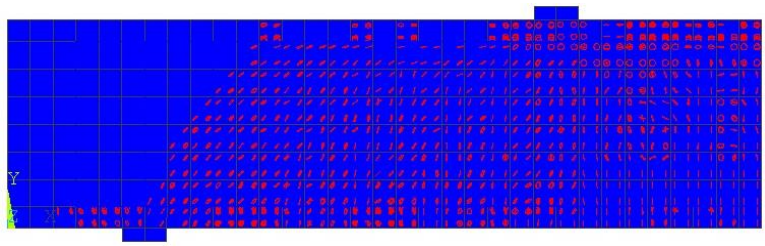

Fig. 12 Numerical crack pattern for, BV1, control beam.

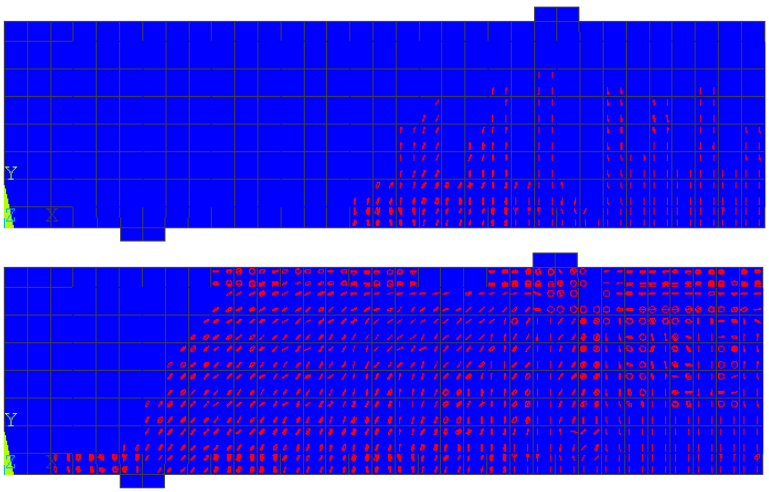

Fig. 13 Numerical evolution of crack pattern for, B1/GFRP, strengthened beam.

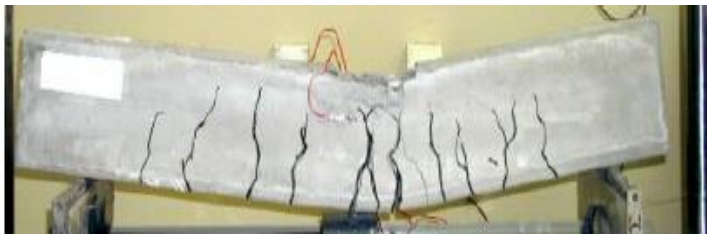

(a) BV1

(b) B1/GFRP/CMAS

Fig. 14 Crack pattern of experimentally tested (a) control and (b) strengthened beams with an anchored GFRP.